

18 **Abstract**

19 Ischemia reperfusion (I/R) injury triggers the activation of coagulation and inflammation processes
20 involved in the pathophysiology of acute kidney injury (AKI). Coagulation proteases upregulated
21 upon renal I/R injury activate protease activated receptors (PARs), which form an important
22 molecular link between inflammation and coagulation. PAR4 is the major thrombin receptor on
23 mouse platelets, and the only PAR that is expressed on both human and murine platelets. In
24 addition, PAR4 is expressed on other cells including podocytes. We here sought to determine the
25 contribution of PAR4 in the host response to renal I/R injury. Hence, we subjected PAR4 knockout
26 and wild-type mice to renal I/R injury. PAR4 knockout mice exhibited an increased tolerance to
27 renal tubular necrosis and showed a decreased neutrophil influx in response to renal I/R,
28 independent from platelet PAR4. On the other hand, PAR4 deficiency resulted in albumin cast
29 formation in peritubular capillaries and showed a tendency towards albuminuria. Transmission
30 Electron Microscopy revealed an increase in podocyte foot process effacement. Our findings
31 suggest that PAR4 contributes to renal injury likely through facilitating neutrophil migration,
32 independent from platelet PAR4. In addition, PAR4 fulfils an important function in the
33 maintenance of podocyte integrity following renal I/R insult. Subsequently, loss of PAR4 results
34 in albuminuria.

35

36

37

38

39 **Introduction**

40 Acute kidney injury (AKI) is a common and costly complication in hospitalized patients, and is
41 independently associated with increased risk of death(1). AKI severity is directly related to patient
42 outcome; even minor changes in serum creatinine predict prognosis in AKI patients after major
43 surgery.(2) Despite the progress in knowledge of the underlying pathophysiology, a recent
44 epidemiological study demonstrated that the incidence of AKI continues to grow.(3) AKI is often
45 triggered by ischemia reperfusion (I/R), which leads to a complex interplay between inflammatory
46 and coagulation processes and renal tissue remodelling(4, 5). More comprehensive understanding
47 of the mechanism underlying these processes is needed to devise strategies to control AKI or
48 accelerate renal recovery. Host-derived coagulation proteases, such as the serine proteases
49 thrombin and factor Xa have been implicated in renal I/R injury(5, 6). Serine proteases regulate
50 haemostasis as well as inflammation and tissue remodelling, thus linking the underlying processes
51 involved in the pathophysiology of AKI(7, 8). Serine proteases elicit cellular effects through
52 cleavage of Protease Activated Receptors (PARs). PARs are a family of seven transmembrane
53 spanning G-protein-coupled receptors that are broadly expressed on immune cells, platelets, and
54 also on renal cells.(9) Upon cleavage, a previously cryptic sequence becomes exposed and acts as
55 a receptor-activated tethered ligand(10), hereby initiating downstream signalling. The PAR family
56 consists of 4 members (PAR1 to PAR4). It has been demonstrated that PAR4 is expressed on
57 podocytes and proximal tubular epithelial cells in both mice and human.(9) Furthermore, PAR4 is
58 the major thrombin receptor on mouse platelets, and the only PAR that is expressed on both human
59 and murine platelets.(11) Although PAR1 and PAR2 have been studied more extensively in context
60 of I/R injury disorders including AKI,(12, 13) the role of PAR4 in the pathophysiology of I/R

61 induced AKI remains largely unknown. Thus, in this study we investigated the effect of PAR4
62 deficiency upon renal I/R.

63

64 **Material and methods**

65

66 **Animals**

67 Specific pathogen-free C57BL/6J mice were purchased from Harlan Sprague-Dawley (Horst, the
68 Netherlands). PAR4KO mice were purchased as embryos from Mutant Mouse Regional Resource
69 Centers and backcrossed 8 times into the C57BL/6J background in the animal research Institute
70 Amsterdam at the Academic Medical Center. Experimental groups were age- and sex-matched, and
71 housed in the animal research Institute Amsterdam facility under standard care. All experiments
72 were conducted with mice of 10 to 12 weeks of age. The Institutional Animal Care and Use
73 Committee of the Academic Medical Center approved all experiments.

74

75 **Murine renal ischemia reperfusion injury**

76 Unilateral renal I/R injury was induced by clamping the left renal artery for 25 minutes followed
77 by a reperfusion phase of 1 day. Renal I/R procedure was performed under general anesthesia (2%
78 isoflurane). For analgesic purposes, mice received a subcutaneous injection of 0.1 mg/kg
79 buprenorphin (Temgesic; Schering-Plough, Brussels, Belgium). The contralateral kidney was used

80 as control. After removal of the clamp, restoration of blood flow was determined by visual
81 inspection. To study the role of PAR4 upon renal I/R injury PAR4 KO (n=8) and WT (n=8) mice
82 were subjected to unilateral renal clamping. To study the role of platelet PAR4 upon renal I/R
83 injury, PAR4KO mice transfused with WT platelets (PAR4KO + WTplt) (n=7) were compared
84 with PAR4KO mice transfused with PAR4KO platelets (PAR4KO + PAR4KO plt) (n=6). WT mice
85 transfused with WT platelets (WT + WTplt) (n=5) were compared WT mice transfused with
86 PAR4KO platelets (WT + PAR4KO plt) (n=8).

87 To sacrifice, mice were anesthetized 2% isoflurane followed by cervical dislocation. Kidneys were
88 either snap-frozen in liquid nitrogen or formalin-fixed followed by paraffin embedment.

89

90 **Platelet isolation and transfusion**

91 To obtain non-activated platelets for transfusion, blood from PAR4KO mice (n=15) and WT mice
92 (n=15) was collected with a 21-G needle from the inferior vena cava and diluted 4:1 with citrate.
93 Blood was centrifuged at room temperature for 15 minutes at 180 g to obtain platelet rich plasma
94 (PRP). PRP was centrifuged at 250 g for 20 minutes in the presence of acid citrate dextrose, 85
95 mM $\text{Na}_3\text{C}_3\text{H}_5\text{O}(\text{COO})_3$, 110 mM Glucose, 65 mM $\text{C}_6\text{H}_8\text{O}_7$); platelet pellets were washed in 6 mL
96 Buffer A (152 mM NaCl, 13.2 mM NaHCO_3 , 6.16 mM Glucose, 1.1 mM $\text{MgCl}_2 \cdot 6\text{H}_2\text{O}$, 2.9 mM
97 KCl, 1mM EDTA, pH6.5). Platelets were re-pelleted and resuspended in 1 mL SSP+ (Storage
98 solution for platelets, Sanquin, Amsterdam, the Netherlands). Platelet count and platelet activation
99 were determined by flow cytometry (FACS Calibur, Becton Dickinson, Franklin Lakes, NJ) using
100 hamster anti-CD61-APC monoclonal antibody (BioLegend, San Diego, CA) and anti-CD62p-FITC

101 (BD Biosciences, San Jose, CA) in accordance with manufacturers' instructions. Platelet
102 transfusates (200 ul $\sim 3 \times 10^7$ / 20 g BW) were administered directly after isolation via the tail vein,
103 two hours before renal I/R. This number of injected mouse platelets corresponds to approximately
104 2% of total platelet count(14).

105

106 **Enzyme-linked immunosorbent assay**

107 Kidneys were homogenized in a lysis buffer containing 150mM NaCl, 15mM Tris, 1mM MgCl₂,
108 1mM CaCl₂, 1% Triton and 1% protease inhibitors. Concentrations of monocyte chemoattractant
109 protein 1 (MCP-1), keratinocyte-derived chemokine (KC), tumor necrosis factor- α (TNF- α), were
110 measured in kidney homogenates by ELISA according to the instructions of the manufacturer
111 (R&D Systems, Abingdon, UK). Mouse myeloperoxidase (MPO) concentrations were measured
112 by ELISA in kidney homogenates (DuoSet DY3667, R&D System, Abingdon). Concentrations of
113 thrombin-antithrombin complexes (TATc) in kidney homogenates were measured according to the
114 manufacturer guidelines using Enzygnost® TAT micro Kit (Siemens Healthcare Diagnostics,
115 Erlangen, Germany). All tissue measurements were corrected for total protein concentration which
116 was measured by incubating 1 μ L of 10 times diluted homogenates for 30 minutes at 37°C in 500 μ L
117 of bicinchoninic acid containing 4% of CuSO₄, absorbance was measured at 570nm. Urine albumin
118 (Bethyl laboratories) levels were determined by ELISA according to the manufacturer's
119 instructions.

120

121 **(Immuno)histochemistry**

122 Murine renal tissue was fixed and processed as described previously.(15) Paraffin embedded
123 sections were used for periodic acid-Schiff diastase (PAS-D) staining and immunohistochemistry.
124 The degree of tubular damage was assessed on PAS-D-stained 4- μ m-thick sections by scoring
125 tubular cell necrosis in 10 non-overlapping high-power fields (magnification 40x) in the
126 corticomedullary junction. The degree of injury was scored by a pathologist in a blinded fashion
127 on a 5-point scale: 0=no damage, 1=10% of the corticomedullary junction injured, 2=10-25%,
128 3=25-50%, 4=50-75%, 5=more than 75%, as described previously(8, 16).

129 To determine platelet accumulation in renal tissue, glycoprotein 1b α (GPIb α) antibody, clone
130 SP219, (dilution 1:200, Spring Bioscience) was used and visualized with 3,3-diaminobenzidine.
131 The percentage of positive anti-GP1balpha staining in 5 non-overlapping fields of magnification
132 20 was quantified using image analysis software Fiji (open- source platform for biological-image
133 analysis). Tissue sections were incubated with specific antibodies for granulocytes (dilution 1:1000
134 fluorescein isothiocyanate-labeled anti-mouse Ly6G (Lymphocyte antigen 6 complex, locus G)
135 mAb; BD Biosciences–Pharmingen, Breda, The Netherlands) and albumin (1:500, ITK
136 diagnostics), followed by incubation with the appropriate biotinylated secondary antibody and
137 subsequently visualized with 3.3-diaminobenzidine. Ly-6G positive cells were counted in 10 non-
138 overlapping fields (magnification x20) in the corticomedullary junction. The surface percentage of
139 positive albumin staining in 10 non-overlapping fields (magnification x20) was quantified using
140 image analysis software FIJI.

141

142 **Ultrastructural analysis**

143 After fixation in Karnovsky buffer (Paraformaldehyde, 8% aq., Glutaraldehyde, 25% aq. 0.2 M
144 Cacodylate, 0.2 M sucrose, distilled H₂O) for 48 h, the material was post-fixed with 1%
145 osmiumtetroxide, the tissue samples were block-stained with 1% uranyl acetate, dehydrated in
146 dimethoxypropane, and embedded in epoxyresin LX-112. Electron microscopy sections were
147 stained with tannic acid, uranyl acetate, and lead citrate, and then examined using a transmission
148 electron microscope (Philips CM10; FEI). Images were acquired using a digital transmission
149 electron microscopy camera (Morada 10–12; Soft Imaging System) using Research Assistant
150 software (RvC). Podocyte effacement was analyzed in a blinded fashion by an experienced
151 nephrologist on multiple randomly taken EM images (magnification x4500) in a
152 semiquantitative fashion on a scale of 0-3.

153

154 **Quantitative polymerase chain reaction**

155 Total RNA was extracted from snap-frozen renal tissue sections with Trizol reagent (Invitrogen,
156 Life Technologies, Breda, the Netherlands) and converted to cDNA. mRNA level was analyzed by
157 qPCR with SYBR green PCR master mix. SYBR green dye intensity was analyzed with linear
158 regression analysis using LinReg PCR software(17). Specific gene expression was normalized to
159 mouse housekeeping gene cyclophilin G or TATA-box binding protein (TBP). The following
160 murine primer sets were used: cyclophilin G (forward 5'-AAGGGAATGGAAGAGGAGGA-3'
161 and reverse 5'-CCCTCTGTTGGCCATTGATA-3'); PAR4KO (forward 5'-
162 GATGTTTCCTGGGCTGGG-3' and reverse 5'-GGTTTTCCAGTCACGACG-3'); PAR4WT
163 (forward 5'- TGATCCTGGCAGCATGTG-3' and reverse 5'-
164 TAGGCTCCATTTCTGATCCACC-3'); TBP (forward 5'-GGAGAATCATGGACCAGAACA-

165 3' and reverse 5'- GATGGGAATTCCAGGAGTCA-3'); MCP-1 (forward 5'-
166 CATCCACGTGTTGGCTCA and reverse 5'-GATCATCTTGCTGGTGAATGAGT-3'); KC
167 (forward 5'-ATAATGGGCTTTTACATTCTTTAACC-3', and reverse 5'-
168 AGTCCTTTGAACGTCTCTGTCC-3'); TNF- α (forward 5'-CTGTAGCCCACGTCGTAGC-3',
169 and reverse 5'-TTGAGATCCATGCCGTTG-3'); Neutrophil gelatinase-associated lipocalin
170 (NGAL) (forward 5'-GCCTCAAGGACGACAACATC -3' and reverse 5'-
171 CTGAACCAATTGGGTCTCGC-3'); Kidney injury molecule-1 (KIM-1) (forward 5'-
172 TGGTTGCCTTCCGTGTCTCT-3' and reverse 5'-TCAGCTCGGGAATGCACAA-3')

173

174 **Statistical analysis**

175 All data sets were tested for their distribution prior to analyses. Differences between experimental
176 groups were determined using Mann-Whitney U test. Statistical analysis on human data was
177 performed using Kruskal Wallis with Dunn's post-hoc testing. Correlations were performed using
178 Spearman's test. All analyses were done using GraphPad Prism version 5.01 (GraphPad Software,
179 San Diego, CA) All data are presented as mean \pm SEM (standard error of the mean). A P-value of
180 <0.05 was considered as statistically significant.

181

182 **Results**

183 **Protease-activated receptor 4 expression and renal thrombin generation upon renal**
184 **ischemia/reperfusion injury.** To determine renal PAR4 expression under physiological conditions

185 and upon renal I/R injury, we quantified PAR4 mRNA levels in kidney tissue samples from WT
186 and PAR4KO mice. Renal tissue from WT mice express PAR4 mRNA under normal conditions
187 and expression did not change upon renal I/R. PAR4KO mice demonstrated absence of renal PAR4
188 mRNA expression under normal condition and upon renal I/R injury, demonstrating successful
189 ablation of PAR4 (Fig 1A). To analyze renal thrombin generation, we measured TAT-c in renal
190 tissue homogenates. Here, we show that renal I/R injury results in renal thrombin generation in
191 both WT and PAR4KO mice (Fig 1B). To test the effect of PAR4 deficiency on intra-renal platelet
192 accumulation following renal I/R, we visualized platelets on renal tissue sections. No difference
193 was detected between WT and PAR4KO mice following renal I/R injury (Fig 1C-E).

194

195 **Fig 1. PAR4 expression and renal thrombin generation upon renal ischemia/reperfusion**
196 **injury.** Relative PAR4 mRNA levels were measured in kidneys of WT sham operated mice (white
197 bar, n=8), WT mice 1 day after renal I/R (black bar, n=8), PAR4KO sham operated mice (white
198 bar, n=8) and PAR4KO mice 1 day after renal I/R (grey bar, n=7). Concentrations of thrombin-
199 antithrombin complexes (TATc) were measured in kidneys of WT sham operated mice (white bar,
200 n=2), WT mice 1 day after renal I/R (black bar, n=8), PAR4KO sham operated mice (white bar,
201 n=2) and PAR4KO mice 1 day after renal I/R (grey bar, n=8). Representative pictures of anti-
202 GPIbalpha stained renal tissue sections 20x magnification, scale bar=100µm of WT mice (C) and
203 PAR4KO mice (D), 24 hours following renal I/R. Percentage of positive GP1ba staining in 5 non-
204 overlapping fields (magnification 20x) was quantified using image analysis software FUJI (E) Data
205 are mean±SEM. *: p<0.05

206

207 **Genetic ablation of protease-activated receptor 4 decreases renal ischemia/reperfusion injury**
208 **but increases protein cast formation.** To evaluate the functions of PAR4 expression following
209 renal I/R, WT and PAR4KO mice were subjected to renal I/R injury. PAR4 deletion resulted in a
210 modest, but significant decrease of renal injury as assessed by PASD scoring (Figs 2A-C). Of note,
211 PAR4 gene ablation did not result in reduced mRNA expression of kidney injury markers KIM-1
212 and NGAL (Figs 2D and E). In addition, we found protein casts, present in the tubular lumen of
213 PAR4 KO mice, but absent in WT mice (Figs 2F-J). Taken together, these results demonstrate that
214 PAR4 plays a dual role in the pathophysiology of renal I/R injury: PAR4 is implicated in the
215 processes leading to renal tissue injury, and plays a role in regulating protein filtration and/or
216 reabsorption following renal I/R insult.

217

218 **Fig. 2. Genetic ablation of PAR4 decreases renal I/R injury but increases protein cast**
219 **formation.** Representative pictures of PAS-D stained renal tissue sections of WT mice subjected
220 to renal I/R with 1 day reperfusion (n=8), 20x magnification, scale bar=100um, (A) and PAR4KO
221 mice subjected to renal I/R with 1 day reperfusion (n=8), 20x magnification, scale bar=100um (B).
222 Score for histopathology of renal tubular damage of WT mice (black bar) and PAR4KO mice (grey
223 bar) subjected to renal I/R injury with 1 day reperfusion (C). Measurement of relative mRNA levels
224 of renal damage marker KIM-1 (D) and NGAL (E) to mouse housekeeping gene cyclophilin G in
225 kidneys of WT sham operated mice (white bar, n=6), WT mice 1 day after renal I/R (black bar,
226 n=8), PAR4KO sham operated mice (white bar, n=8) and PAR4KO mice 1 day after renal I/R (grey
227 bar, n=8). Representative pictures of PAS-D stained renal tissue sections (n=8), 10x magnification,
228 scale bar=100um, of WT mice sham operated (n=8) (F), WT mice after 1 day renal I/R (n=8) (G),
229 PAR4KO mice sham operated (n=8) (H), PAR4KO mice after 1 day renal I/R (n=8) (I).

230 Quantification of positive protein casts in 10 non-overlapping (magnification 10x) was quantified
231 (J). Data are mean \pm SEM. *: $p < 0.05$, **: $p < 0.01$, ****: $p < 0.0001$

232
233 **Protease-activated receptor 4 deletion reduces leukocyte infiltration.** Inflammation plays a
234 pivotal role in the pathology of renal I/R injury.(18) Since PAR4 activation modulates several
235 aspects of inflammation including leukocytes recruitment(19), we next explored whether PAR4
236 deletion decreases inflammation following renal I/R injury. Histological examination of WT and
237 PAR4KO kidneys demonstrated a significant reduction of granulocyte influx in kidneys from
238 PAR4 KO mice (Figs 3A-C). However, enzymatic assay for determining granulocyte activity by
239 measuring MPO did not show differences between WT and PAR4 KO (Fig 3D).

240 To further assess the extent of inflammation, we measured the expression of proinflammatory
241 cytokines MCP-1, KC and TNF- α on mRNA and protein level. PAR4 KO mice showed a trend
242 towards increased TNF- α mRNA expression following renal I/R, while the other cytokines and
243 chemokines were not different (Figs 3 E-J). Since PAR4 is the major thrombin receptor on mouse
244 platelets,(11) we hypothesized that platelet PAR4 might influence renal injury and granulocyte
245 influx in our mouse model. However, transfusion of $\sim 3 \times 10^7 / 20$ g/BW (corresponding to
246 approximately 2% of total platelet count in C57BL/6 mice(14)) PAR4KO platelets and WT
247 platelets in PAR4KO mice or WT mice did not affect renal injury following renal I/R (S1A and
248 S1B Figs). Likewise, transfusion of $\sim 3 \times 10^7 / 20$ g/BW PAR4KO platelets and WT platelets in
249 PAR4KO mice or WT mice did not influence renal granulocyte influx (S1C and S1D Figs). Taken
250 together, these results indicate that murine PAR4 plays an important role in neutrophil tissue influx

251 upon renal I/R injury, which was not influenced by platelet transfusion of approximately 2%
252 PAR4KO or WT platelets of total platelet count.

253
254 **Fig. 3. PAR4 deletion reduces leukocyte infiltration.** Representative pictures of neutrophil (Ly6-
255 G positive) stained renal tissue sections (20x magnification, scale bar=100 μ m) of mice WT mice
256 (n=8) (A) and PAR4KO mice (n=8) (B) after 1 day renal I/R. Quantification of positive Ly6G
257 staining in 10 non-overlapping (20x magnification) (C). Concentration of MPO (D) measured by
258 ELISA in kidney homogenates from WT sham operated mice (white bar, n=8), WT mice 1 day
259 after renal I/R (black bar, n=8), PAR4KO sham operated mice (white bar, n=8) and PAR4KO mice
260 1 day after renal I/R (grey bar, n=8). Measurement of inflammatory cytokine monocyte
261 chemoattractant protein 1 (MCP1) (E & F), keratinocyte chemoattractant (KC) (G & H), tumor
262 necrosis factor- α (TNF- α) (I & J) mRNA expression and protein exposure in renal tissue from WT
263 sham operated mice (white bar, n=8), WT mice 1 day after renal I/R (black bar, n=8), PAR4KO
264 sham operated mice (white bar, n=8) and PAR4KO mice 1 day after renal I/R (grey bar, n=8). Data
265 are mean \pm SEM. *: p<0.05, **: p<0.01

266
267 **Genetic ablation of protease-activated receptor 4 in mice results in increased albuminuria**
268 **and loss of podocyte structural integrity upon renal ischemia reperfusion.** Albuminuria is
269 shown to be an independent mediator of progressive kidney damage.(20) The presence of protein
270 casts in PAR4KO mice upon renal I/R suggests ongoing albumin leakage. To evaluate albuminuria,
271 we collected urine to determine the albumin/creatinine ratio (ACR). In addition, we stained renal
272 sections for albumin to confirm that the observed protein casts consist of albumin. PAR4KO mice

273 show a trend towards increased ACR after I/R (Figure 4A). Under normal conditions, WT and
274 PAR4KO mice did not show any albuminuria. Albumin staining on renal sections demonstrates
275 the presence of albumin in the protein casts (Figure 4B, C), which is significantly increased in
276 PAR4KO compared to WT mice following renal I/R injury (Figure 4D).

277 To investigate whether the origin of albuminuria lies in the glomerular filter, we assessed the
278 glomeruli of PAR4KO and WT mice by transmission electron microscopy to investigate
279 ultrastructural differences. No structural podocyte abnormalities were encountered in both sham-
280 treated WT and PAR4 KO mice (S2 Fig). However, upon renal I/R PAR4KO deficient mice
281 demonstrated a significantly increased loss of podocyte structure integrity as reflected by extensive
282 foot process effacement (Figure 4E-G). Since the origin of albumin leakage can also be found in
283 the proximal tubular reabsorption machinery, in which endocytic receptor megalin plays an
284 important role in albumin reabsorption,(21, 22) we evaluated the tubular expression of albumin
285 reabsorption receptor megalin by immunostainings. No differences were found (data not shown).
286 Taken together these results imply that PAR4 is implicated in maintaining podocyte integrity upon
287 renal I/R insult.

288

289 **Fig. 4. Genetic ablation of PAR4 in mice results in increased albuminuria and loss of podocyte**
290 **structural integrity upon renal I/R.** Measurement of albumin creatinine ration in WT sham
291 operated mice (white bar, n=7), WT mice 1 day after renal I/R (black bar, n=8), PAR4KO sham
292 operated mice (white bar, n=8) and PAR4KO mice 1 day after renal I/R (grey bar, n=8) (A).
293 Representative pictures of albumin staining in WT (B) and PAR4KO (C) mice 1 day after renal
294 I/R. Quantification of positive albumin casts in 10 non-overlapping (magnification 10x, scale bar=
295 100 μ m) (D). Representative electron micrographs of podocytes surrounding a glomerular capillary

296 in WT mouse (E) and PAR4KO (F) mouse (magnification 4500x, scale bar= 2 μ m) after 1 day renal
297 I/R (arrows point to podocyte effacements). Podocyte effacement semi-quantitative score on a scale
298 of 0-3, on multiple randomly taken EM images (magnification 4500x) in WT and PAR4KO mice
299 after 1 day renal I/R (G). Data are mean \pm SEM. *: p<0.05, **: p<0.01, ***: p<0.001

300

301 **Discussion**

302 AKI is a common and costly complication frequently caused by ischemia reperfusion (I/R)
303 injury,(1) leading to a complex interplay between inflammatory and coagulation processes and
304 renal tissue remodelling.(4, 23) Serine proteases such as thrombin and factor Xa regulate
305 haemostasis as well as inflammation and tissue remodelling, and have been associated with renal
306 I/R injury(5, 6). The cellular effects of serine proteases are elicited by cleaving of PAR's,
307 comprising of PAR1-4(10) which are widely expressed on myeloid cells and various renal cells.(9)
308 Recently it has been shown that PAR4 deficiency offers protection against acute I/R injury in
309 cerebral and heart tissue.(24, 25) To date the role of PAR4 upon renal I/R is unknown. Here we
310 sought to determine the role of PAR4 in the host response to renal I/R injury. Our main finding is
311 that genetic ablation of PAR4 gene decreases renal necrosis and leukocyte influx in the
312 corticomedullary region, independent from platelet PAR4. In addition, following renal I/R injury,
313 PAR4 deficiency resulted in intra-tubular albumin casts and albuminuria, likely through loss of
314 podocyte structural integrity. Taken together these results suggest that PAR4 is involved in the
315 pathophysiology of renal I/R injury enabling leukocytes influx into renal tissue. On the other hand,
316 PAR4 also fulfils a functional role in the maintenance of podocyte structure upon renal I/R injury
317 insult.

318 In a study of Kolpakov et al, it was shown that PAR4 is involved in pathophysiology of myocardial
319 I/R.(24) They showed that PAR4 expression in WT mice is upregulated in heart tissue following
320 acute myocardial I/R and demonstrated that ablation of the PAR4 gene results in smaller heart
321 infarct size and decreased myocyte death. In correspondence with this model, the study of Mao et
322 al demonstrated that in a mouse model of cerebral I/R injury, PAR4 deficiency attenuated I/R
323 injury.(25) In contrast to the study of Kolpakov et al, WT mice in our renal I/R mouse model did
324 not show increased renal PAR4 expression upon I/R. In line with Kolpakov et al. and Mao et al.,
325 we demonstrated that PAR4KO mice show less renal tissue injury following renal I/R when
326 compared to WT mice. However, albeit significant, the difference was modest between PAR4KO
327 and WT mice, which may explain why mRNA expression levels of kidney damage markers KIM-
328 1 and NGAL did not differ between WT mice and PAR4KO mice.

329 PAR4 has been shown to be involved in acute inflammatory responses.(26) Vergenolle et al.
330 showed that PAR4 agonists cause neutrophil rolling and adherence, indicating that PAR4 activation
331 contribute to the recruitment of neutrophils.(19) Migration of neutrophils into renal parenchyma is
332 a significant component in the pathophysiology of renal I/R injury.(18, 27) Neutrophils can
333 aggravate kidney injury by releasing proteases such as myeloperoxidase, reactive oxygen species
334 or NETS(16, 28, 29). In this study, we show that PAR4 deficient mice demonstrate less neutrophil
335 accumulation in the renal parenchyma, indicating that PAR4 plays a role in neutrophil recruitment
336 following renal I/R. To note, PAR4KO did not impact the expression of pro-inflammatory cytokine
337 MCP-1 or KC upon renal I/R, suggesting that PAR4 is more involved in the processes facilitating
338 neutrophil rolling and adherence rather than the renal inflammatory cytokine response. Activated
339 platelets play an important role in facilitating granulocyte influx upon AKI(30, 31) by forming a
340 bridge to the endothelial wall, stimulating granulocyte rolling and adherence.(32) Murine platelets

341 are dependent on PAR4 for thrombin-induced signaling and subsequent activation.(33) We
342 therefore speculated that platelet PAR4 is important for thrombin dependent platelet activation
343 upon AKI and subsequently neutrophil tissue influx and renal injury in our model. However, PAR4
344 deficiency did not influence platelet accumulation upon renal I/R. In accordance with the study
345 performed by Huo et al. showing that injection of $\sim 3 \times 10^7 / 20$ g/BW activated WT platelets
346 increased leukocyte arrest on the surface of atherosclerotic lesions, we transfused PAR4KO and
347 WT mice with $\sim 3 \times 10^7 / 20$ g/BW PAR4KO or WT platelets prior to renal I/R injury. However,
348 $\sim 3 \times 10^7 / 20$ g/BW corresponding to approximately 2% of total platelet count did not affect renal
349 injury or granulocyte renal influx. This suggests that murine platelet PAR4 is not implicated in the
350 pathophysiology of AKI in our model. However, it may also indicate that more than 2% transfused
351 PAR4KO or WT platelets of total platelet count in mice is needed to affect the neutrophil influx
352 and renal tissue injury. Taken together these results suggest that PAR4 is involved in the
353 pathophysiology of renal injury, possibly through facilitating neutrophil tissue influx, independent
354 of renal cytokine release.

355 Madhusudhan et al. demonstrated that PAR4 is expressed on podocytes in both mice and human(9,
356 34), however its function is unknown so far. Podocytes are essential in the maintenance of an intact
357 glomerular filtration barrier and podocyte stress and/or injury is a major cause of albuminuria(35,
358 36). Strikingly, we here demonstrated for the first time that PAR4 deficiency results in albumin
359 cast formation in the peritubular capillaries. In addition, PAR4 deficient mice show a tendency
360 towards elevated albumin levels in urine following renal I/R, hinting at a problem with the
361 glomerular filtration barrier. Under normal conditions, podocyte structure is characterized by their
362 interdigitated foot processes that are wrapped around the glomerular capillaries and form filtration
363 slits which are bridged by the slit diaphragm.(37) Upon stress or injury the podocytes' structure can

364 be altered, leading to podocyte foot process effacement, which causes albuminuria.(38) In this
365 study, transmission electron microscopy of the glomeruli revealed increased levels of podocytes
366 foot process effacement in PAR4 deficient mice subjected to renal I/R, suggesting that PAR4 is
367 involved in maintenance of a normal structure of podocytes upon I/R injury. Loss of podocyte
368 PAR4 makes podocytes more susceptible to structural changes upon I/R insult, resulting in
369 increased albumin leakage.

370 In conclusion, our data shows that PAR4, is implicated in the pathophysiology of renal injury,
371 likely through facilitating neutrophil influx. In addition, PAR4 is involved in maintaining podocyte
372 integrity following renal I/R insult. To what extent platelet specific PAR4 is implicated needs to be
373 further explored in future studies.

374

375 **References**

- 376 1. Chertow GM, Burdick E, Honour M, Bonventre JV, Bates DW. Acute kidney injury, mortality,
377 length of stay, and costs in hospitalized patients. *J Am Soc Nephrol.* 2005;16(11):3365-70.
- 378 2. Lassnigg A. Minimal Changes of Serum Creatinine Predict Prognosis in Patients after
379 Cardiothoracic Surgery: A Prospective Cohort Study. *Journal of the American Society of*
380 *Nephrology.* 2004;15(6):1597-605.
- 381 3. Hsu RK, McCulloch CE, Dudley RA, Lo LJ, Hsu CY. Temporal changes in incidence of dialysis-
382 requiring AKI. *J Am Soc Nephrol.* 2013;24(1):37-42.
- 383 4. Bonventre JV, Yang L. Cellular pathophysiology of ischemic acute kidney injury. *J Clin Invest.*
384 2011;121(11):4210-21.
- 385 5. Thuillier R, Favreau F, Celhay O, Macchi L, Milin S, Hauet T. Thrombin inhibition during kidney
386 ischemia-reperfusion reduces chronic graft inflammation and tubular atrophy. *Transplantation.*
387 2010.
- 388 6. Tillet S, Giraud S, Kerforne T, Saint-Yves T, Joffrion S, Goujon JM, et al. Inhibition of coagulation
389 proteases Xa and IIa decreases ischemia–reperfusion injuries in a preclinical renal transplantation
390 model. *Translational research.* 2016.
- 391 7. Esmon CT. The interactions between inflammation and coagulation. *Br J Haematol.*
392 2005;131(4):417-30.

- 393 8. Lattenist L, Jansen MPB, Teske G, N. C, J.C. M, A.R. R, et al. Activated protein C protects against
394 renal ischaemia/reperfusion injury, independent of its anticoagulant properties. *Thromb*
395 *Haemost* 2016;116(1):124-33.
- 396 9. Madhusudhan T, Kerlin BA, Isermann B. The emerging role of coagulation proteases in kidney
397 disease. *Nature reviews*. 2016.
- 398 10. Coughlin S. Thrombin signalling and protease-activated receptors. *Nature*. 2000.
- 399 11. French SL, Hamilton JR. Protease-activated receptor 4: from structure to function and back again.
400 *Br J Pharmacol*. 2016.
- 401 12. Sevastos J, Kennedy SE, Davis DR, Sam M, Peake PW, Charlesworth JA, et al. Tissue factor
402 deficiency and PAR-1 deficiency are protective against renal ischemia reperfusion injury. *Blood*.
403 2007;109:577-83.
- 404 13. Jesmin S, Gando S, Zaedi S, Prodhon SH, Sawamura A, Miyauchi T, et al. Protease-activated
405 receptor 2 blocking peptide counteracts endotoxin-induced inflammation and coagulation and
406 ameliorates renal fibrin deposition in a rat model of acute renal failure *Shock*. 2009.
- 407 14. Barrios M R-AA, Gil A, Salazar AM, Taylor P, Sánchez EE, Arocha-Piñango CL, Guerrero B.
408 Comparative hemostatic parameters in BALB/c, C57BL/6 and C3H/He mice. *Thromb Res*.
409 2009;124(3):338-43.
- 410 15. Stokman G, Leemans JC, Claessen N, Weening JJ, Florquin S. Hematopoietic stem cell
411 mobilization therapy accelerates recovery of renal function independent of stem cell
412 contribution. *J Am Soc Nephrol*. 2005;16(6):1684-92.
- 413 16. Jansen MP, Emal D, Teske GJ, Dessing MC, Florquin S, Roelofs JJ. Release of extracellular DNA
414 influences renal ischemia reperfusion injury by platelet activation and formation of neutrophil
415 extracellular traps. *Kidney Int*. 2016.
- 416 17. Ruijter JM, Ramakers C, Hoogaars WM, Karlen Y, Bakker O, van den Hoff MJ, et al. Amplification
417 efficiency: linking baseline and bias in the analysis of quantitative PCR data. *Nucleic Acids Res*.
418 2009;37(6):e45.
- 419 18. Bonventre JV, Zuk A. Ischemic acute renal failure- An inflammatory disease? *Kidney international*.
420 2004.
- 421 19. Vergnolle N, Derian CK, D'Andrea MR, Steinhoff M, Andrade-Gordon P. Characterization of
422 Thrombin-Induced Leukocyte Rolling and Adherence: A Potential Proinflammatory Role for
423 Proteinase-Activated Receptor-4. *The Journal of Immunology*. 2002;169(3):1467-73.
- 424 20. Gorriz JL, Martinez-Castelao A. Proteinuria: detection and role in native renal disease
425 progression. *Transplantation reviews*. 2012.
- 426 21. Nielsen R, Christensen EI. Proteinuria and events beyond the slit. *Pediatr Nephrol*.
427 2010;25(5):813-22.
- 428 22. Cui S, Verroust PJ, Moestrup SK, Christensen EI. Megalin/gp330 mediates uptake of albumin in
429 renal proximal tubule. *Am J physiol*. 1996.
- 430 23. Eltzschig HK, Eckle T. Ischemia and reperfusion--from mechanism to translation. *Nat Med*.
431 2011;17(11):1391-401.
- 432 24. Kolpakov MA, Rafiq K, Guo X, Hooshdaran B, Wang T, Vlasenko L, et al. Protease-activated
433 receptor 4 deficiency offers cardioprotection after acute ischemia reperfusion injury. *Journal of*
434 *Molecular and Cellular Cardiology*. 2016;90:21-9.
- 435 25. Mao Y, Zhang M, Tuma RF, Kunapuli SP. Deficiency of PAR4 attenuates cerebral
436 ischemia/reperfusion injury in mice. *J Cereb Blood Flow Metab*. 2010;30(5):1044-52.
- 437 26. Fu Q, Cheng J, Gao Y, Zhang Y, Chen X, Xie J. Protease-Activated Receptor 4- A Critical Participator
438 in Inflammatory Response. *Inflammation*. 2015;38.

- 439 27. Awad AS, Rouse M, Huang L, Vergis AL, Reutershan J, Cathro HP, et al. Compartmentalization of
440 neutrophils in the kidney and lung following acute ischemic kidney injury. *Kidney Int.*
441 2009;75(7):689-98.
- 442 28. Saffarzadeh M, Juenemann C, Queisser MA, Lochnit G, Barreto G, Galuska SP, et al. Neutrophil
443 extracellular traps directly induce epithelial and endothelial cell death: a predominant role of
444 histones. *PLoS One.* 2012;7(2):e32366.
- 445 29. Mayadas TN, Cullere X, Lowell CA. The multifaceted functions of neutrophils. *Annu Rev Pathol.*
446 2014;9:181-218.
- 447 30. Singbartl K, Forlow SB, Ley K. Platelet, but not endothelial, P-selectin is critical for neutrophil-
448 mediated acute postischemic renal failure. *FASEB J.* 2001;15:2337-44.
- 449 31. Jansen MPB, Florquin S, Roelofs J. The role of platelets in acute kidney injury. *Nat Rev Nephrol.*
450 2018.
- 451 32. Ed Rainger G, Chimen M, Harrison MJ, Yates CM, Harrison P, Watson SP, et al. The role of
452 platelets in the recruitment of leukocytes during vascular disease. *Platelets.* 2015;26(6):507-20.
- 453 33. Hamilton JR, Cornelissen, I., and Coughlin, S.R. . Impaired hemostasis and protection against
454 thrombosis in protease-activated receptor 4-deficient mice is due to lack of thrombin signaling in
455 platelets. *Journal of thrombosis and haemostasis.* 2004;2:1429-35.
- 456 34. Madhusudhan T, Wang H, Straub BK, Grone E, Zhou Q, Shahzad K, et al. Cytoprotective signaling
457 by activated protein C requires protease-activated receptor-3 in podocytes. *Blood.*
458 2012;119(3):874-83.
- 459 35. Johnstone DB, Holzman LB. Clinical impact of research on the podocyte slit diaphragm. *Nat Clin*
460 *Pract Nephrol.* 2006.
- 461 36. Benzing T. Signaling at the Slit Diaphragm. *Journal of the American Society of Nephrology.*
462 2004;15(6):1382-91.
- 463 37. Brinkkoetter PT, Ising C, Benzing T. The role of the podocyte in albumin filtration. *Nat Rev*
464 *Nephrol.* 2013;9(6):328-36.
- 465 38. Kriz W, Shirato I, Nagata M, LeHir M, Lemley KV. The podocyte's response to stress: the enigma
466 of foot process effacement. *Am J Physiol Renal Physiol.* 2013;304(4):F333-47.

467

468 **Supporting information**

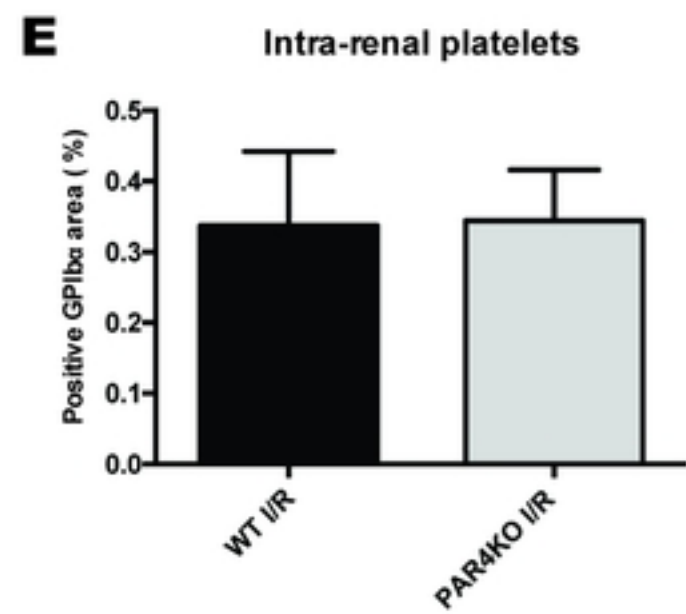
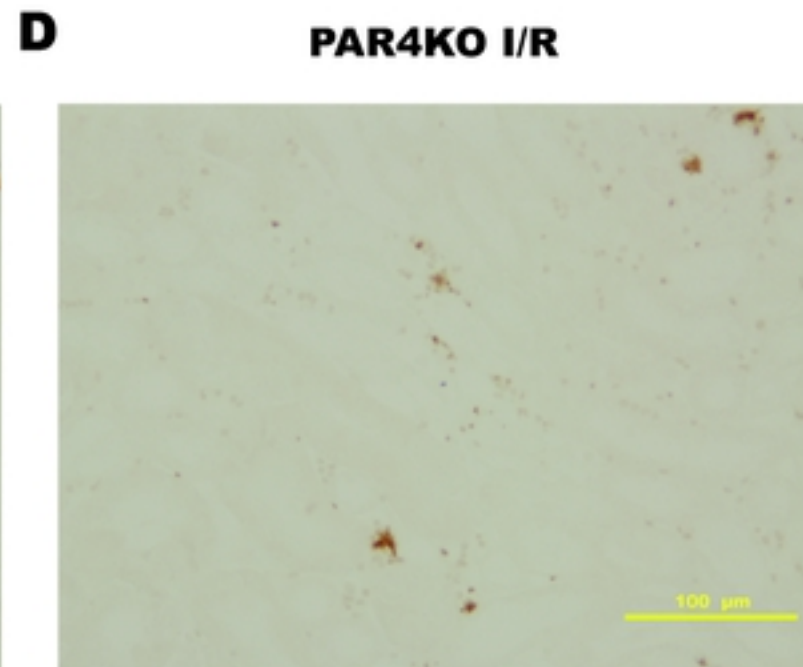
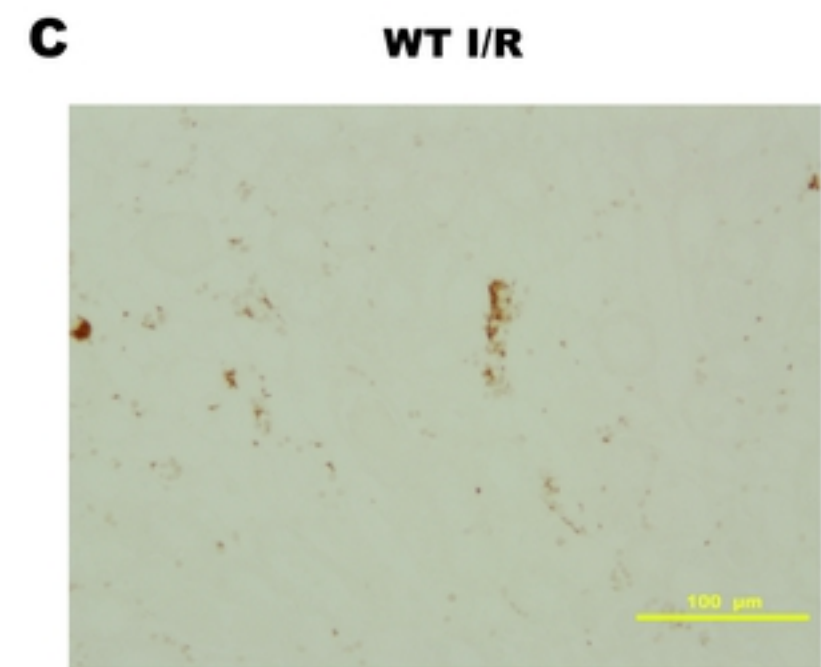
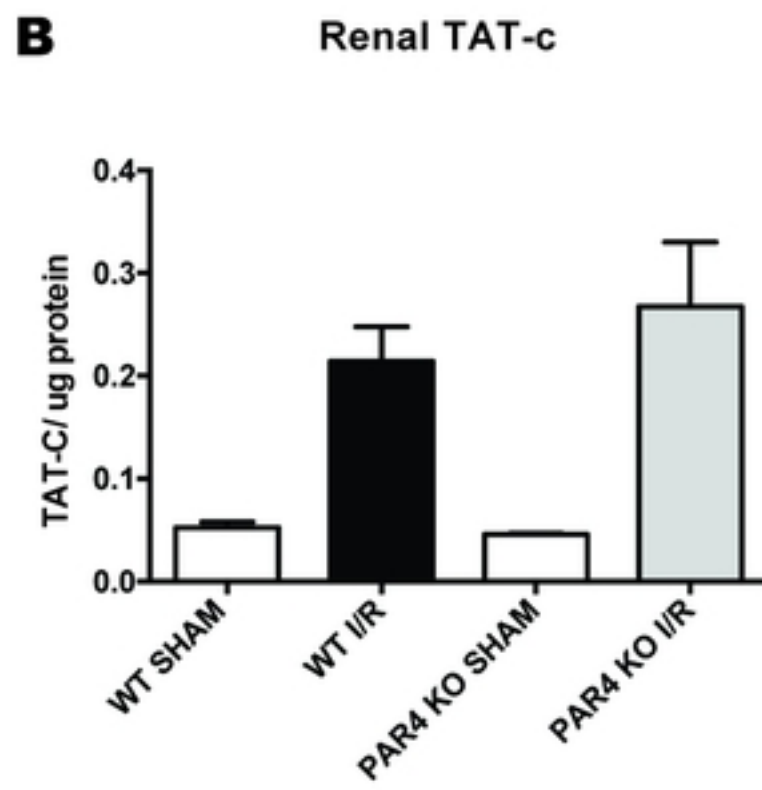
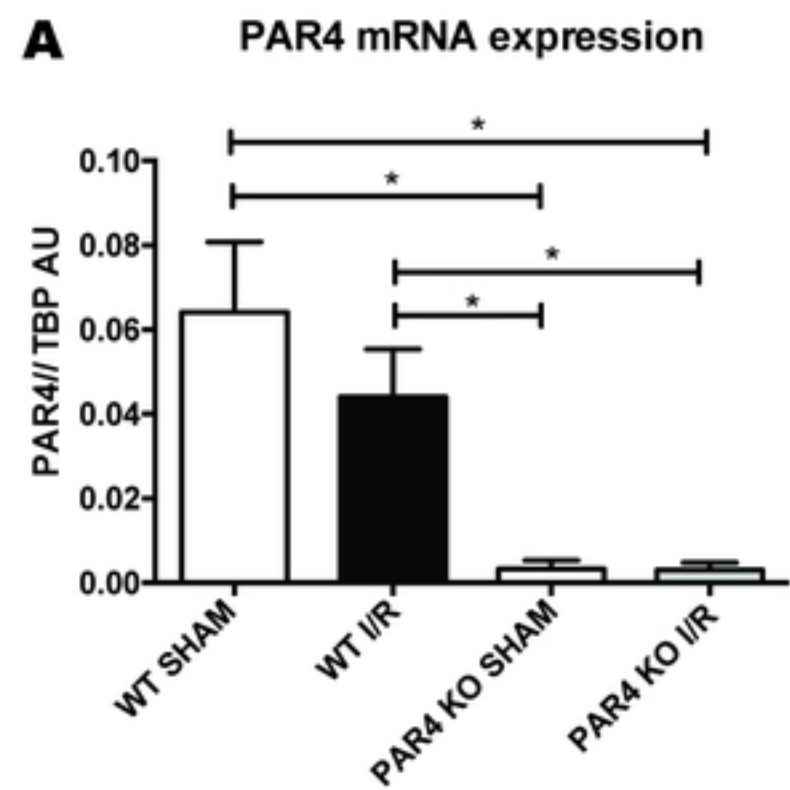
469 **S1 Fig.** Representative electron micrographs of podocytes surrounding a glomerular capillary in
470 WT mouse (E) and PAR4KO (F) mouse (magnification 4500x, scale bar= 2µm) sham-operated
471 (arrows point to podocytes).

472 **S2 Fig.** Representative pictures of PAS-D stained renal tissue sections (magnification 40x, scale
473 bar= 50 µm) and score of histopathology of renal tubular damage of: PAR4KO mice transfused
474 with $\sim 3 \times 10^7 / 20$ g/BW WT platelets (black bar) or PAR4KO platelets (grey bar) (A), WT mice

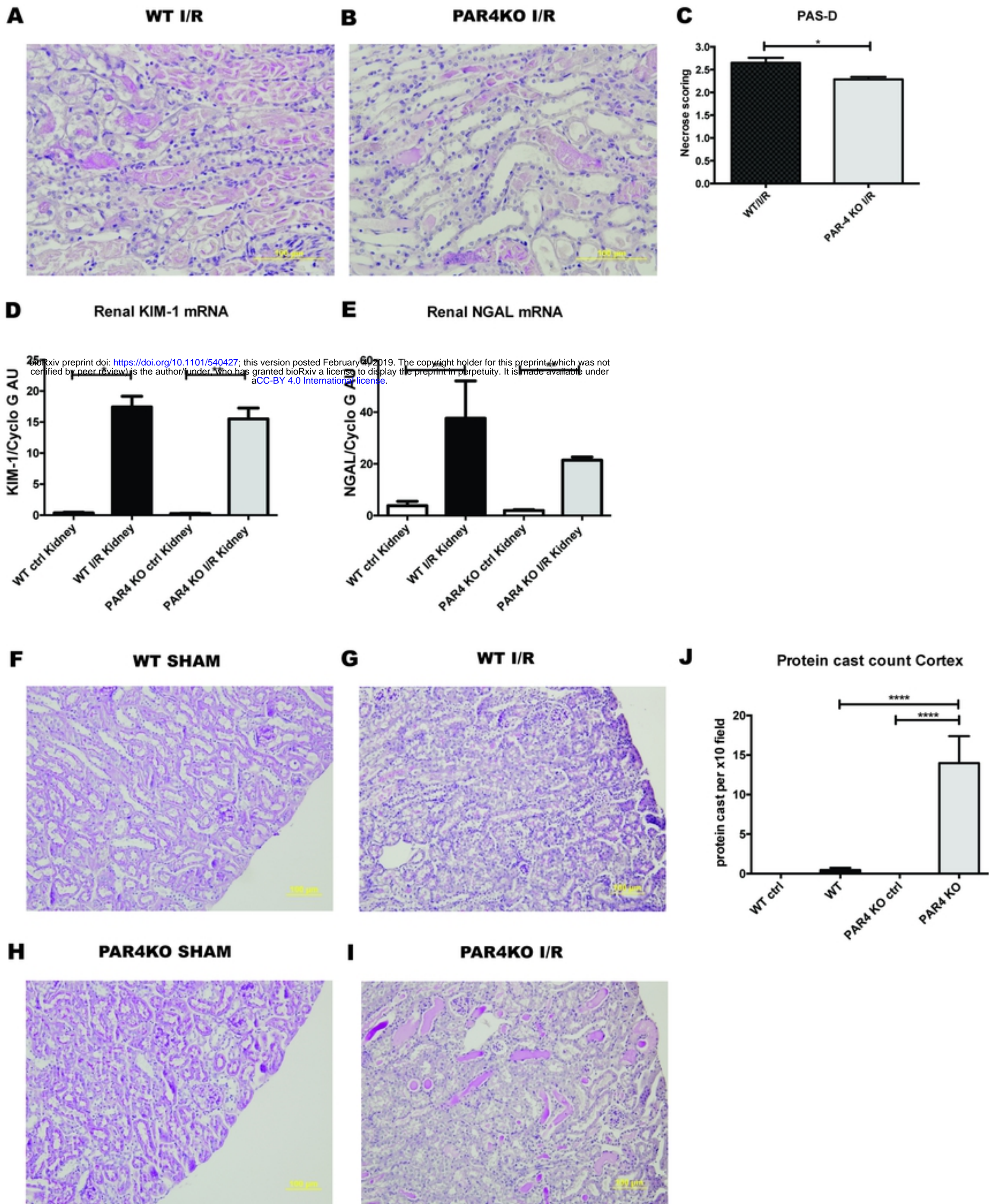
475 transfused with $\sim 3 \times 10^7 / 20$ g/BW WT platelets (black bar) or PAR4KO platelets (grey bar) (B).
476 Representative pictures of neutrophil (Ly6-G positive) stained renal tissue sections (magnification
477 40x, scale bar=50 μ m) and quantification of positive Ly6G staining in 10 non-overlapping high
478 power fields (magnification 40X) in PAR4KO mice transfused with $\sim 3 \times 10^7 / 20$ g/BW WT platelets
479 (black bar) or PAR4KO platelets (grey bar) (C), WT mice transfused with $\sim 3 \times 10^7 / 20$ g/BW WT
480 platelets (black bar) or PAR4KO platelets (grey bar) (D).

481

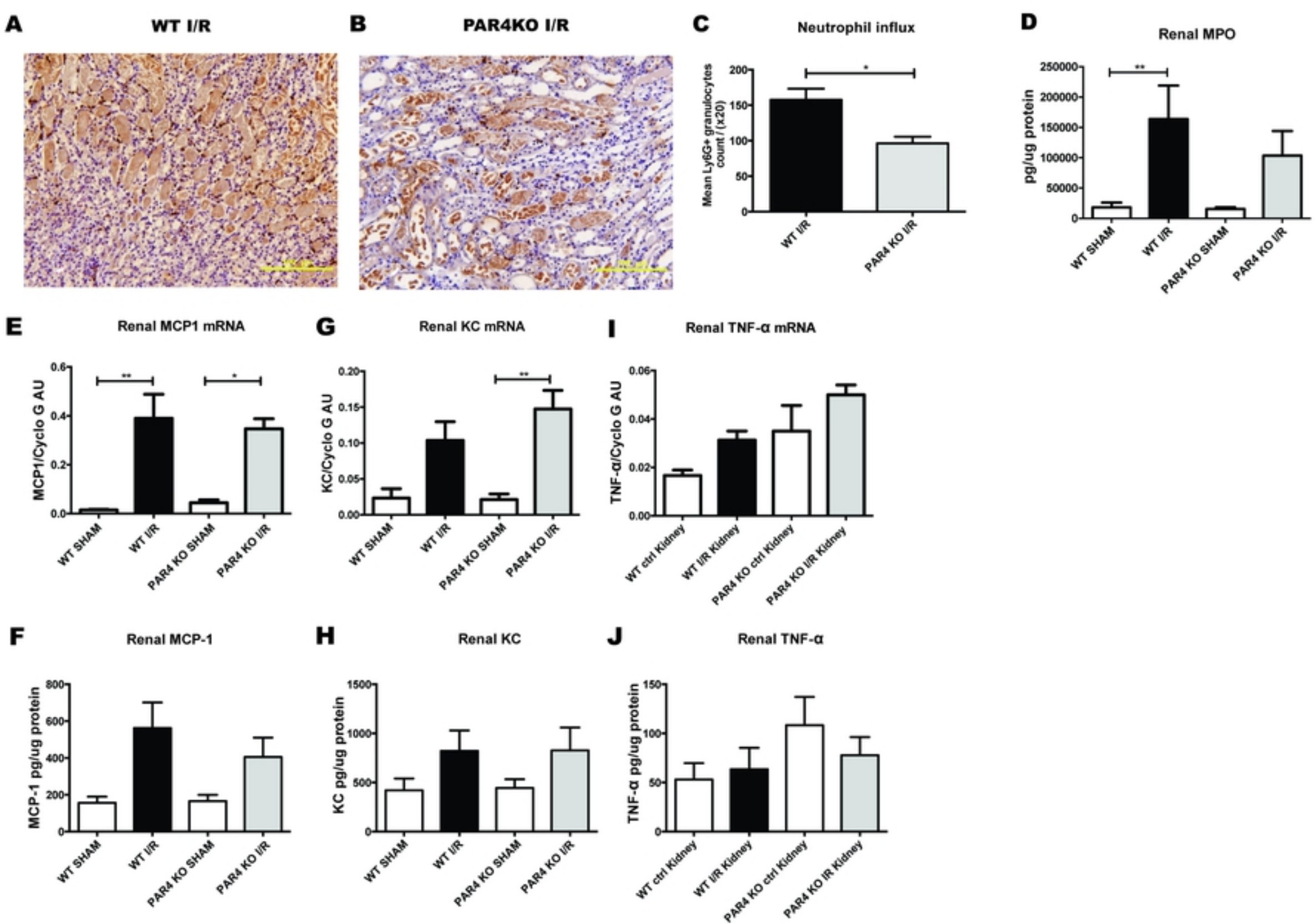
482



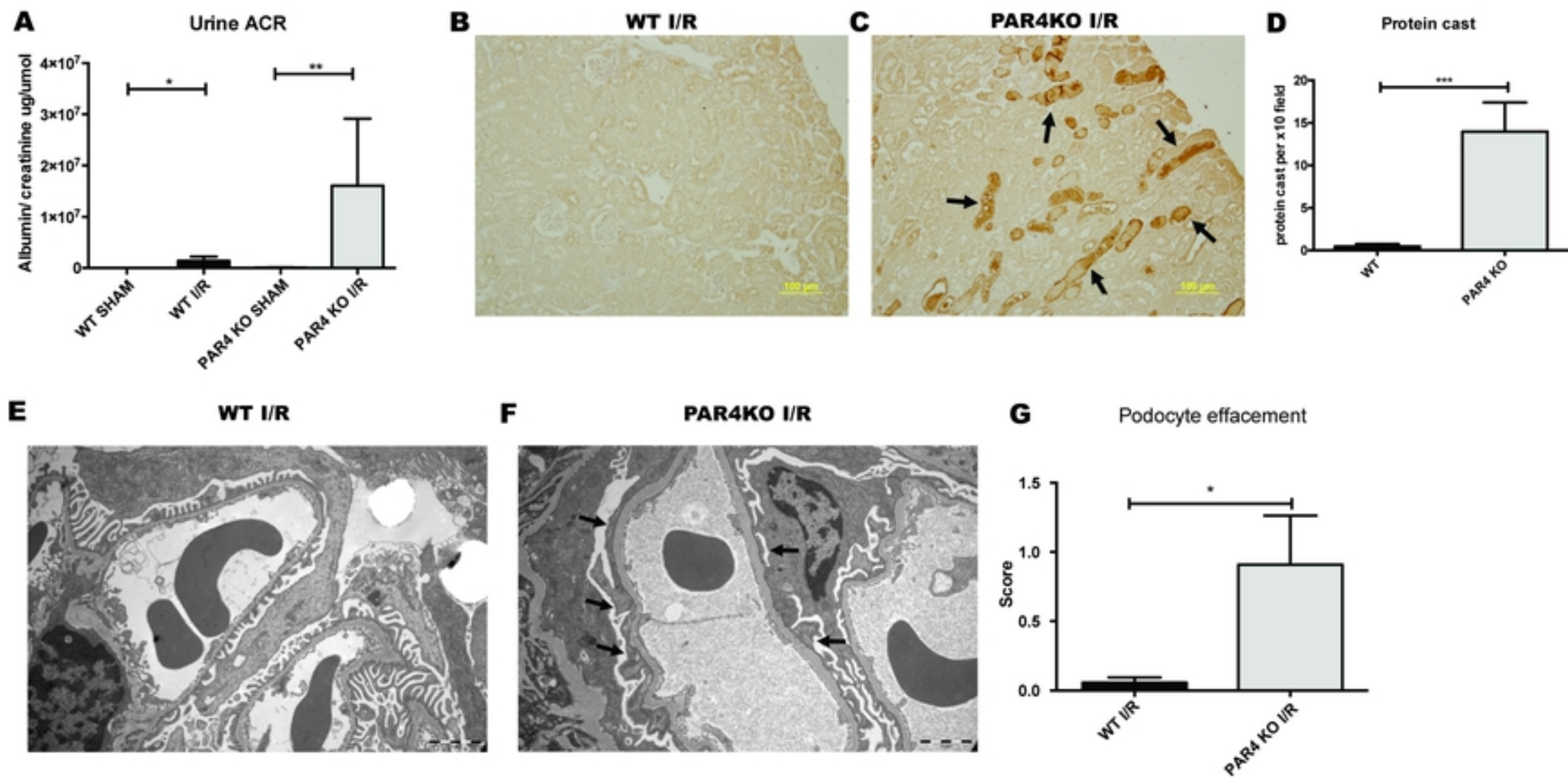
Figure



Figure



Figure



Figure